arXiv:physics/0504006v1 [physics.optics] 1 Apr 2005

Modeling of a Resonant Tunneling Diode Optical Modulator

J. J. N. Calado and J. M. L. Figueiredo*
Departamento de Física, Faculdade de Ciências e Tecnologia,
Universidade do Algarve, Campus de Gambelas, 8005-139 Faro, Portugal

C. N. Ironside
Department of Electronics and electrical Engineering, University of Glasgow G12 8LT, UK

The integration of a double barrier resonant tunneling diode within a unipolar optical waveguide provides electrical gain over a wide bandwidth. Due to the non-linearities introduced by the double barrier resonant tunneling diode an unipolar InGaAlAs/InP optical waveguide can be employed both as optical modulator and optical detector. The modeling results of a device operating as optical modulator agree with preliminary experimental data, foreseeing for an optimized device modulation depths up to 23 dB with chirp parameter between -1 and 0 in the wavelength range analyzed (1520 nm - 1600 nm).

Keywords: Modeling, resonant tunneling diodes, optical waveguide, optical Modulation.

I. INTRODUCTION

Due to their high-speed response and radio frequency (rf) gain, several groups have proposed the application of resonant tunnelling diodes (RTDs) in the optical and infrared domains [1].

A novel optoelectronic device based on the integration of a RTD with an optical waveguide (OW), the RTD-OW, as been proposed for electro-optical and opto-electrical conversion [2]. The waveguide configuration is used to ensure large interaction volume between the RTD regions and the guided light. The full demonstration and development of this new device concept in the ternary AlGaAs/GaAs and quaternary InGaAlAs/InP material systems can be of great importance for optical communication, specially in high-speed fibre radio links. The AlGaAs/GaAs material system is interesting for short hall communications in the wavelength range around 900 nm, and the InGaAlAs/InP material system is useful in the wavelength range where optical fibres have the lowest loss and chromatic dispersion (1300 nm to 1600 nm).

Our group has successfully integrated AlGaAs and InGaAlAs RTDs within unipolar AlGaAs/GaAs and InGaAlAs/InP optical waveguides, respectively, and demonstrated optical modulation of guided light around 900 nm and 1550 nm [3][4]. In this paper we report modeling results of the device operating as an electro-optical converter at 1550 nm, confirms preliminary experimental data [4][5].

II. PRINCIPLE OF OPERATION AS A MODULATOR

Essentially, the RTD-OW is a unipolar device consisting of a double barrier quantum well (DBQW) resonant tunneling diode (RTD) embedded within a ridge channel optical waveguide. The DBQW-RTD structure consists of two AlAs barriers surrounding a InGaAs quantum well. The optical waveguide comprehends two moderately n-doped InGaAlAs layers lattice matched to InP, sandwiched between highly n-doped InP cladding regions, Fig. 1.

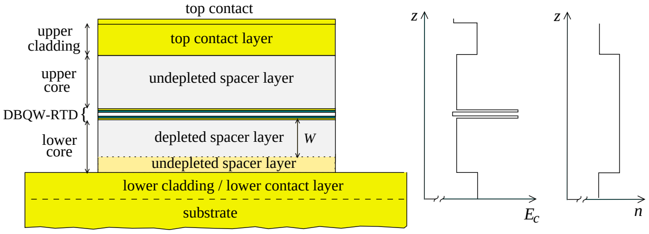

FIG. 1: Schematic diagram of the RTD-OW wafer structure, Γ-conduction band-edge and refractive index profiles.

The presence of the DBQW-RTD within the waveguide core introduces high nonlinearities in the current-voltage (I-V) characteristic of the unipolar waveguide: the device I-V curve shows large negative differential resistance (NDR), Fig. 2. The physics that gives rise to this type of I-V is explained in [4].

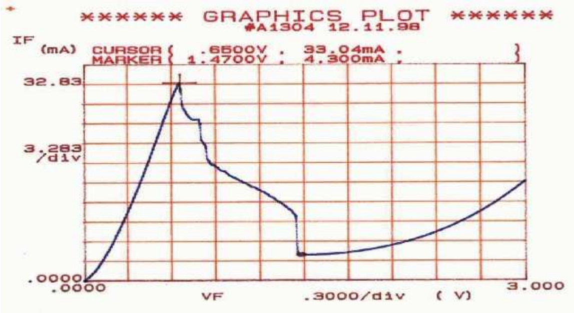

FIG. 2: Experimental current-voltage characteristic of an InGaAlAs/InP RTD-OW.

---

*Electronic address: jlongras@ualg.pt

As a consequence of the presence of the RTD within the unipolar waveguide core a non-uniform potential distribution is induced across the waveguide cross-section, Fig. 3. The magnitude of the associated electric field distribution depends strongly on the bias voltage. When the device operating point switches from the peak to the valley regions of the I-V curve there is an enhancement of the electric field across the waveguide depletion region. This produces substantial changes in the absorption coefficient of the waveguide at wavelengths near the core material band-edge via the Franz-Keldysh effect (for more details see [4]). The operation of the RTD-OW as an optical modulator takes advantage of this absorption change induced by the RTD peak-to-valley switching.

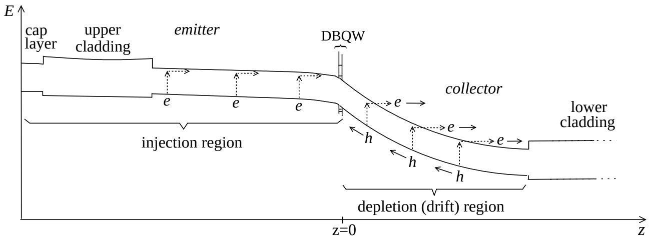

FIG. 3: Schematic diagram of the energy bands in a RTD-OW at the valley voltage as a function of distance: upper curve is the lowest conduction band energy and the lower curve represents the highest valence band energy. The light absorption occurs mainly in the device depletion region.

Preliminary experimental results indicate that a non-optimized device designed to act as a modulator is capable of high-speed modulation (up to 26 GHz) with extinction ratio higher than 10 dB over a wide range of wavelengths at driving power as low as 7.7 dBm, Fig. 4 [5].

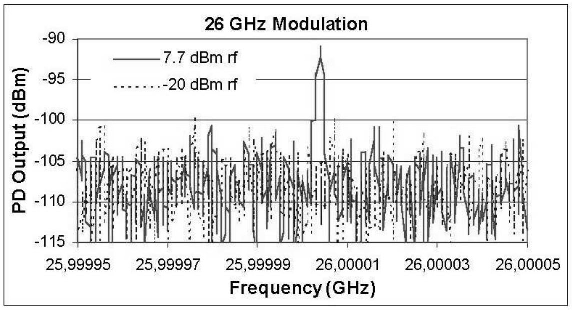

FIG. 4: Electrical spectra of optical signals modulated at 26 GHz for driving powers of -20 dBm and +7.7 dBm.

III. DEVICE MODELING PHASES

The device modeling comprehends two phases. In the first, the electrical characteristics of the device such as the I-V curve and the potential distribution across the waveguide cross-section are determined. In the second part, the waveguide optical properties induced changes such as the extinction coefficient and the refractive index variations at different bias voltage and as function of the guided light wavelength are calculated.

The RTD-OW electrical modelling employs the WinGreen simulation package [6] that determines the device I-V characteristic and the potential profiles across the waveguide cross-section as function of the applied bias. The I-V curve permits to extract the NDR region characteristics: the peak and the valley voltages, Fig. 5.

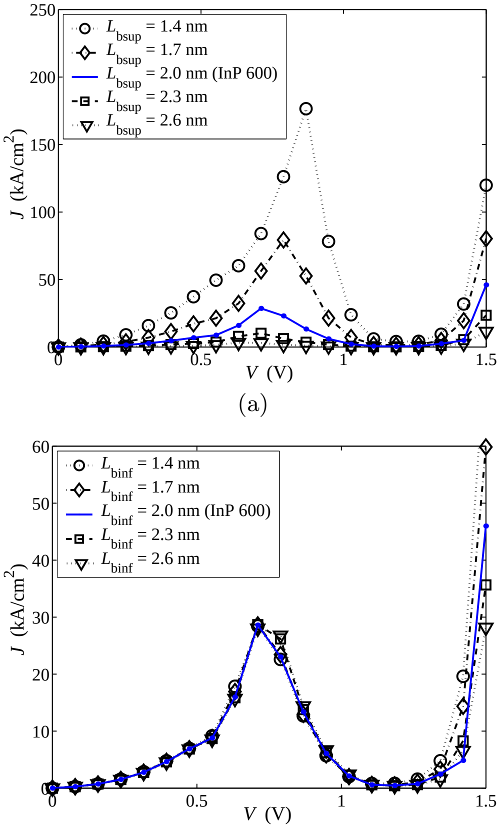

(a)

(b)

FIG. 5: Typical device I-V characteristics determined by the WinGreen simulation package for several barrier thickness: a) emitter barrier and b) collector barrier (see Fig. 3).

The electric field distribution $F(z)$ across the waveguide for a given bias voltage V, Fig. 6b), is obtained through the gradient of the potential distribution, Fig. 6a).

The waveguide absorption coefficient at a given voltage V is then determined as a function of the electric field distribution $F(z)$, in V/cm, and of the light energy E, in eV, using the Franz-Keldysh relation [7],

$$\alpha(E,F) = \sum_j A_j F^{\frac{1}{3}} \left[\left| \left(\frac{d\mathrm{Ai}}{dz} \right)_{\beta_j} \right|^2 - \beta_j \left| \mathrm{Ai}(\beta_j) \right|^2 \right], \tag{1}$$

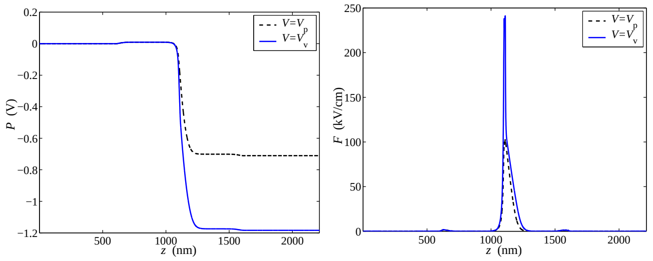

(a) (b)

FIG. 6: The device typical potential distributions at the peak and the valley voltages a) and the corresponding electric field distributions b).

where Ai is the Airy function, $A_j = 7,65 \times 10^5 C(2m_{rj}/m_0)^{\frac{4}{3}}/nE$, $\beta_j = B_j(E_g - E)F^{-\frac{2}{3}}$, $B_j = 1,1 \times 10^5(2m_{rj}/m_0)^{\frac{1}{3}}$, E_g is the core band-gap energy expressed in eV, and n is the refractive index; m_{rj} and m_0 are the electron-hole reduced effective mass and electron rest mass, respectively; C is a scaling parameter to adjust Eq. 1 to independent experimental data [7]. The sum is over the light and heavy holes.

The absorption change due to the RTD peak to valley switching is then given by:

$$\Delta\alpha(\hbar\omega, \Delta F_{p-v}) = \alpha(\hbar\omega, F_v) - \alpha(\hbar\omega, F_p), \tag{2}$$

where $F_{p,v}$ represents the magnitude of the electric field at the peak (p) and at the valley (v), respectively.

The refractive index change as function of the bias is determined from the absorption change through the Kramers-Kronig relation [7]

$$\Delta n(\hbar\omega, F) = \frac{\hbar c}{\pi} \int_0^\infty \frac{\Delta\alpha(\hbar\omega', F)}{(\hbar\omega')^2 - (\hbar\omega)^2} d\omega', \tag{3}$$

The modulation depth is estimated through

$$R_{on-off}(\text{dB}) = 4,343\gamma_f \Delta\alpha, \tag{4}$$

where γ_f represents the overlap integral between the electric field and the optical field distributions. The chirp parameter is calculated using the relation

$$\alpha_H = \Delta n / \Delta k, \tag{5}$$

where k is the extinction coefficient, given by $\Delta k = \Delta\alpha\lambda/4\pi$.

IV. MODELING RESULTS

The objective of this work is to understand the role of the structural and material parameters on the device performance in order to determine the optimized device structure for each application. The study reported here aims the determination of the RTD-OW structure that gives the highest modulation depth with the minimum propagation loss. To achieve this purpose it is necessary to maximize the electric field change when the device operation point switches from the peak to the valley region and the overlap between the electric field distribution and the guided mode.

According the modeling results, the optimized modulator structure corresponds to a RTD-OW configuration consisting of two 2 nm thick AlAs barriers surrounding a 6 nm thick InGaAlAs quantum well, symmetrically embedded within a 300 mm unipolar InGaAlAs waveguide core with doping concentration of 1×10^{16} cm^{-3} and 600 nm thick InP cladding layers highly doped (2×10^{18} cm^{-3}). A 200 μm long RTD-OW shows extinction ratio up to 23 dB around 1560 nm with chirp parameter of -0.25, Fig. 7. The results also show the propagation loss are considerable higher than the "best" values reported in the literature. The way to decrease the propagation loss are under current investigation.

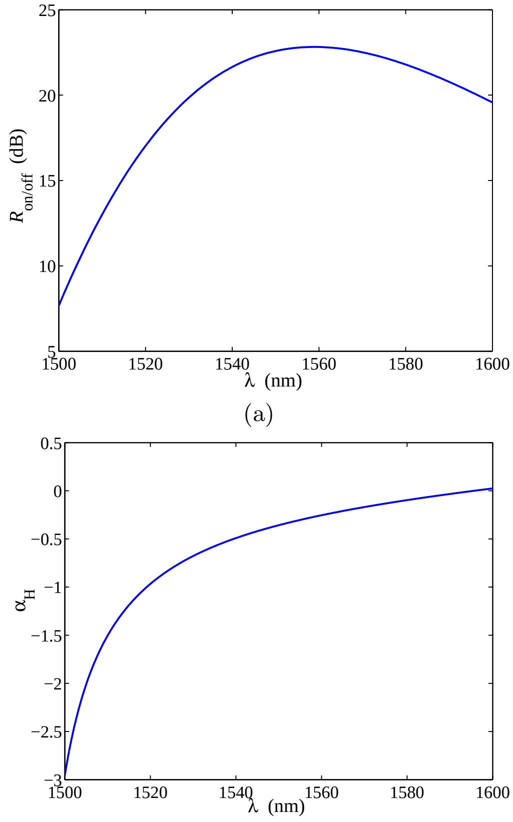

(a)

(b)

FIG. 7: (a) Extinction ratio $R_{\text{on/off}}$ and (b) chirp parameter α_{H} as function of the wavelength induced by the peak-to-valley switching.

The refractive index change and the extinction coefficient variation are shown in Fig. 8, and appears to indicate the RTD-OW has high potential to operate as an electro-refraction modulator through an interferometer configuration.

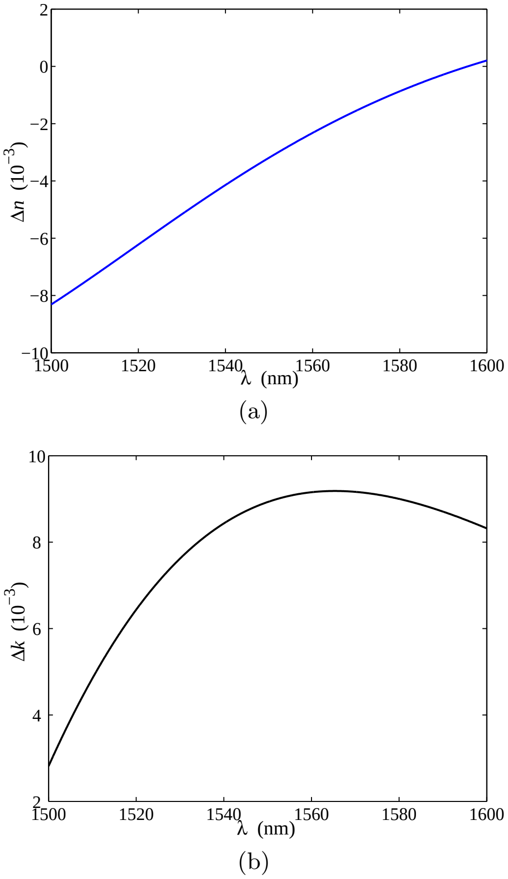

FIG. 8: (a) Refractive index variation Δn and (b) extinction coefficient change Δk as function of the wavelength induced by the peak-to-valley switching.

V. CONCLUSION AND FUTURE WORK

The modeling results corroborate preliminary modulation depth experimental data [4][5]. The fabrication of devices based on the present optimized structures is being considered.

The current devices also show detection capabilities. Its is foreseen the device can operate as a light detector incorporating an intrinsic integrated amplifier for the photocurrent generated by the incident light. The presented model is currently being extended to include the effect of light absorption.

Acknowledgment

This work is supported by the Fundação para a Ciência e a Tecnologia (Portugal) under Grant No. POSI/41760/CPS/2001.

[1] I. Gravé, S. C. Kan, G. Griffel, S. W. Wu, A. Sa'ar, and A. Yariv, "Monolithic integration of a resonant tunneling diode and a quantum well semiconductor laser," Appl. Phys. Lett., Vol. 58, pp. 110-112, 1991; K. Sano, K. Murata, T. Akeyoshi, N. Shimizu, T. Otsuji, M. Yamamoto, T. Ishibashi and E. Sano,"Ultra-fast optoelectronic circuit using resonant tunnelling diodes and uni-travelling-carrier photodiode," Electron. Lett., Vol. 34, pp. 215-217, 1998.

[2] S.G. McMeekin, M.R. Taylor, B. Vogele, C.R. Stanley, C.N. Ironside, "Franz-Keldysh effect in a optical waveguide containing a resonant tunnelling diode," *Appl. Phys. Lett.*, Vol. 65, pp. 1076-1078, 1994.

[3] J. M. L. Figueiredo, C. R. Stanley, A. R. Boyd, C. N. Ironside, S. G. McMeekin, and A. M. P. Leite, *Optical modulation in a resonant tunneling relaxation oscillator*, *Appl. Phys. Lett.*, Vol. 74, pp. 1197-1199, 1999.

[4] J. M. L. Figueiredo, C. N. Ironside, and C. R. Stanley, "Electric field switching in a resonant tunnelling diode electroabsorption modulator," *IEEE J. Quant. Electron.*, Vol. 37, pp. 1547-1552, 2001.

[5] J. M. L. Figueiredo, C. N. Ironside, and C. R. Stanley, "Ultralow voltage resonant tunnelling diode electroabsorption modulator," *J. Modern Optics*, Vol. 49, pp. 939-945, 2002.

[6] The WinGreen simulation package, http://www.fz-juelich.de/isg/mbe/software.html.

[7] S.L. Chuang, *Physics of Optoelectronic Devices*, Wiley & Sons 1995.